Neurobiology of Disease 170 (2022) 105752

Contents lists available at ScienceDirect

Neurobiology of Disease

journal homepage: www.elsevier.com/locate/ynbdi

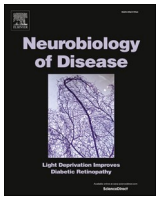

Effects of Eph/ephrin signalling and human Alzheimer's disease-associated EphA1 on *Drosophila* behaviour and neurophysiology

Edgar Buhl [a,*], Yoon A. Kim [b,c], Tom Parsons [a], Bangfu Zhu [a], Ismael Santa-Maria [b,c], Roger Lefort [b,c], James J.L. Hodge [a]

[a] School of Physiology, Pharmacology and Neuroscience, University of Bristol, University Walk, Bristol BS8 1TD, UK
[b] Taub Institute for Research on Alzheimer's Disease & the Aging Brain, Columbia University, New York, NY, USA
[c] Department of Pathology & Cell Biology, Columbia University, New York, NY, USA

ARTICLE INFO

Keywords:
Alzheimer's disease
Ca^{2+} imaging
Circadian rhythms
Drosophila melanogaster
Electrophysiology
Eph/ephrin signalling
Locomotor activity
Longevity
Memory
Sleep

ABSTRACT

Alzheimer's disease (AD) is the most prevalent neurodegenerative disease placing a great burden on people living with it, carers and society. Yet, the underlying patho-mechanisms remain unknown and treatments limited. To better understand the molecular changes associated with AD, genome-wide association studies (GWAS) have identiffed hundreds of candidate genes linked to the disease, like the receptor tyrosine kinase EphA1. However, demonstration of whether and how these genes cause pathology is largely lacking. Here, utilising fiy genetics, we generated the ffrst *Drosophila* model of human wild-type and P460L mutant EphA1 and tested the effects of Eph/ephrin signalling on AD-relevant behaviour and neurophysiology. We show that EphA1 mis-expression did not cause neurodegeneration, shorten lifespan or affect memory but flies mis-expressing the wild-type or mutant receptor were hyper-aroused, had reduced sleep, a stronger circadian rhythm and increased clock neuron activity and excitability. Over-expression of endogenous fly Eph and *RNAi*-mediated knock-down of Eph and its ligand ephrin affected sleep architecture and neurophysiology. Eph over-expression led to stronger circadian morning anticipation while ephrin knock-down impaired memory. A dominant negative form of the GTPase Rho1, a potential intracellular effector of Eph, led to hyper-aroused flies, memory impairment, less anticipatory behaviour and neurophysiological changes. Our results demonstrate a role of Eph/ephrin signalling in a range of behaviours affected in AD. This presents a starting point for studies into the underlying mechanisms of AD including interactions with other AD-associated genes, like Rho1, Ankyrin, Tau and APP with the potential to identify new targets for treatment.

1. Introduction

Alzheimer's disease (AD) is the most common neurodegenerative disorder with ~30 million people living with it worldwide, rapidly increasing with aging populations (Lane et al., 2018). It is mainly characterised by cognitive decline and premature death caused by neurodegeneration, accompanied by disruptions in many different cellular systems and molecular processes. The best studied neuropathological hallmarks of AD include the abnormal cleavage of the amyloid precursor protein (APP) leading to aggregation of cytotoxic extracellular β-amyloid (Aβ) oligomeric plaques and intracellular accumulation of hyperphosphorylated microtubule associated protein Tau (MAPT) as neuroffbrillary tangles (NFTs) (Lane et al., 2018). Age is the biggest risk factor for AD with the majority of cases being sporadic, associated with a range of contributing genetic, epigenetic and environmental risk factors. Genome-wide association studies (GWAS) identiffed several genes associated with late onset Alzheimer's disease (LOAD) including common variants of the receptor tyrosine kinase EphA1 (Carrasquillo et al., 2011; Hollingworth et al., 2011; Naj et al., 2011) and, more recently, in Caribbean Hispanic families (also nominally signiffcant in Caucasians), identiffed a nonsynonymous variant proline to leucine substitution at the highly conserved protein coding

Abbreviations: AD, Alzheimer's disease; CS+, conditioned stimulus; CS-, unconditioned stimulus; C_V, spike ffring irregularity index; DAM, *Drosophila* activity monitor; DD, continuous darkness; EAI, evening anticipation index; Eph, erythropoietin-producing hepatocellular receptor tyrosine kinase; EphA1, human Eph receptor A1; ephrin, Eph receptor interacting protein; GWAS, genome-wide association study; LD, 12h:12h light:dark conditions; LOAD, late onset Alzheimer's disease; l-LNv, large lateral ventral clock neurons; MAI, morning anticipation index; MB, mushroom body; MCH, 4-methylcyclohexanol; OCT, 3-octanol; PDF, pigment dispersing factor; PI, performance index; R_{in}, input resistance; RMP, resting membrane potential; RS, rhythmic statistics; SFR, spontaneous ffring rate; ZT, zeitgeber time.

* Corresponding author.
E-mail address: e.buhl@bristol.ac.uk (E. Buhl).

https://doi.org/10.1016/j.nbd.2022.105752
Received 18 June 2021; Received in revised form 9 April 2022; Accepted 9 May 2022
Available online 13 May 2022

position 460 (P460L) (Vardarajan et al., 2015).

Despite EphA1 being the ffrst identiffed of the Eph receptor family (Hirai et al., 1987), it remains the least characterised, therefore posing the question of its potential patho-mechanism. Activation of EphA1 by its GPI membrane-anchored ligand ephrin-A leads to contact-dependent, bi-directional signalling of the adjacent cells but, additionally, Eph receptors can interact with other cell-surface receptors and signal independently of ephrin ligands (Lisabeth et al., 2013). Eph/ephrin signalling plays an important role for developmental morphogenesis, organogenesis, axonal guidance, mediating cell migration, cell fate determination and synaptic plasticity (Lai and Ip, 2009; Klein, 2012). Furthermore, disturbance of Eph/ephrin signalling is associated with oncogenesis (Pasquale, 2010) as well as immune dysregulation and infiammation (Ieguchi, 2015) potentially relating changes in EphA1 signalling to neuro-infiammation, a common, but poorly understood, pathological feature of AD (Ransohoff, 2016). Indeed, EphA1 has been implicated in regulating the neuroinfiammatory process and affecting AD progression (Villegas-Llerena et al., 2016). The EphA1 P460L mutation is believed to lead to increased receptor clustering potentially resulting in a constitutively active receptor (Kim et al., 2021), affecting intracellular signalling via Rho and Ras family GTPases and Akt/mTORC1 activity, in particular, increasing the balance of RhoA versus Rac1 (Lisabeth et al., 2013).

The fruit fiy D. melanogaster is an established model of human disease due to its short life cycle, cheap and easy maintenance, genetic tractability and molecular conservation with approximately 75% of the human disease-causing genes having a close fiy orthologue (Bier, 2005). Furthermore, it has well-studied neuroanatomy, genetics, physiology and behaviour that are useful for studying disease. We and others have successfully studied aspects of AD in fiies (Chen et al., 2014; Tabuchi et al., 2015; Dissel et al., 2017; Papanikolopoulou et al., 2019) and shown effects of Tau, Aβ (Buhl et al., 2019; Higham et al., 2019a) and the membrane cytoskeleton anchor of ion channels and transporters Ankyrin (Higham et al., 2019b) on physiology and behaviour. Eph/ephrins form phylogenetically conserved families of receptors and ligands, with a large expansion in gene number in humans but with only a single Eph receptor (Scully et al., 1999) and ligand (Bossing and Brand, 2002) in *Drosophila*, making the fly a tractable model to study its actions. Similar to mammals, where EphA1 is highly expressed during development and in the adult brain (Flanagan and Vanderhaeghen, 1998; Pasquale, 2008), *Drosophila* Eph and ephrin are likewise expressed in the embryonic developing (Scully et al., 1999; Bossing and Brand, 2002) and adult central nervous system (Boyle et al., 2006).

Here we characterise the effects of AD-associated EphA1 and investigate the role of Eph/ephrin signalling on disease relevant behaviour and physiology using *Drosophila*. We generated flies that allow targeted mis-expression of the human wild-type ($EphA1^{WT}$) and P460L mutant EphA1 ($EphA1^{P460L}$). We assess the role of Eph/ephrin signalling using tissue speciffc *RNAi*-mediated knock-down of fly Eph (Eph^{RNAi}) and ephrin ($ephrin^{RNAi}$), over-expression of fiy endogenous Eph (*Eph*), mis-expression of human $EphA1^{WT}$ and $EphA1^{P460L}$ and knock-down of the receptor interactor Rho1 ($Rho1^{DN}$), the *Drosophila* homologue of human RhoA. We test the effects of these genotypes on neurodegeneration, lifespan, locomotion, memory, circadian rhythms and sleep as well as on neurophysiological properties.

2. Results

2.1. Generation of human EphA1 expressing fiies

The transgenic fiies used in this study were generated using the *PhiC31* integrase system that facilitates sequence-specific recombination between two attachment sites, *attB* and *attP*, sharing a 3 bp region where crossover takes place (Bateman et al., 2006). This method allows selection of the site of integration for the transgene of interest. Genotyping and sequencing conffrmed the presence of the inserted transgenes, integrated into chromosome 2 (EphA1 wild-type ($EphA1^{WT}$) and EphA1 bearing P460L mutation ($EphA1^{P460L}$); see Methods, Supplementary Fig. S1A, B). To regulate expression of the transgenes, we utilized the *Gal4/UAS* system, which uses the yeast *Gal4* transcription factor to activate transcription of the transgene under control of the upstream activator sequence (*UAS*) promoter element (Brand and Perrimon, 1993; Duffy, 2002). This allows for tissue-speciffc expression of the transgene by crossing speciffc *Gal4* lines with transgenic lines where the transgene is under *UAS* control. We verified the efficiency of the knock-down for the ephrin ligand ($elav > ephrin^{RNAi}$, 34% *mRNA* decrease) and the Eph receptor ($elav > Eph^{RNAi}$, 54% *mRNA* decrease) as well as the efficiency of the over-expression of fly endogenous Eph ($elav > Eph$, 152% *mRNA* increase) transgenes using RT-qPCR by expressing the transgenes throughout the nervous system (*elav-Gal4*) and sampling whole fly heads (Supplementary Fig. S1C).

2.2. EphA1 mis-expression affects fiy climbing performance

A hallmark feature of Alzheimer's disease (AD) is neurodegeneration and early death (Lane et al., 2018). We have shown in fiies that expressing human *MAPT* (*Tau*) or *Aβ42* in the developing and adult eye causes photoreceptor degeneration leading to a 'rough eye' phenotype, while pan-neuronal over-expression shortens lifespan (Higham et al., 2019b). Mis-expression of the human wild-type receptor $EphA1^{WT}$, the mutated receptor $EphA1^{P460L}$ or a dominant-negative form of the GTP-binding protein Rho1 ($Rho1^{DN}$) throughout development and adulthood in photoreceptor neurons (*GMR-Gal4*) had no effect on size or organisation of the compound eyes that displayed the normal regular array of ommatidia like wild-type controls (Fig. 1A). Likewise, while both ephrin and its receptor Eph are expressed in the developing fiy visual system (Dearborn et al., 2012), *RNAi*-mediated knock-down of ephrin or Eph, or over-expression of fly endogenous Eph did not alter the appearance of the eyes. We next tested whether expressing these genes pan-neuronally (*elav-Gal4*) would affect the general health of the animals by measuring lifespan (Fig. 1B and **Supplementary** Table S1). The median survival of mated female control fiies (*Gal4 / +*) was 44 days and all the other parental controls (*UAS / +*) had a similar lifespan. Again, neither knock-down nor over- and mis-expression of any of the tested genes resulted in a significantly altered survival. Remarkably, even expression of $Rho1^{DN}$, while producing fewer offspring, did not affect longevity of the fiies in our hands (44 d) despite earlier reports of lethality (Fritz and VanBerkum, 2002). Thus, manipulation of Eph/ephrin signalling or mis-expression of human EphA1 did not lead to speciffc neurodegeneration or early death.

Since neuronal and synaptic loss in AD typically manifests ffrst in the hippocampus (Lane et al., 2018) leading to cognitive impairment and behavioural deffcits including motor dysfunction (Beauchet et al., 2015), we tested whether Eph/ephrin manipulation effected locomotor ability by utilising the negative geotaxis refiex (Fig. 1C) that is disrupted in fiy AD models (Higham et al., 2019b). Over 71% of young wild-type and *UAS*-control flies climbed to the top of a tube within 10 s after startling by tapping them to the bottom (Fig. 1D and **Supplementary** Table S1). Pan-neuronal (*elav-Gal4*) down-regulation of Eph or ephrin or Eph over-expression did not significantly alter this response although Eph^{RNAi} fiies climbed worse (56%) but failing to reach statistical signiffcance. $EphA1^{WT}$ and $EphA1^{P460L}$ mis-expressing and $Rho1^{DN}$ fiies showed a hyperarousal phenotype by surpassing the controls at this task with over 90% of the fiies climbing to the top. Climbing performance of all fiies sharply decreased after about 2 weeks with $EphA1^{WT}$, $EphA1^{P460L}$ and $Rho1^{DN}$ fiies maintaining their hyperarousal and consistently outscoring controls and Eph/ephrin knock-down fiies alike (Supplementary Fig. S2A, B and **Supplementary** Table S1). Only fiy Eph over-expressor fiies reached a similar level at the last measured time point (4 weeks old) but so did their respective UAS controls. Since not all of the tested fly lines were in the same genetic background and since fly behavioural assays can be sensitive to background effects, we outcrossed all *UAS* and the *elav-Gal4* strains to Canton S w- flies and repeated the climbing assay with these flies verifying our original findings (Supplementary Fig. S2C). In summary, targeted mis-expression of both human EphA1 receptors did not result in gross neurodegeneration or shortened lifespan but, along with $Rho1^{DN}$, led to a lasting increase in climbing performance.

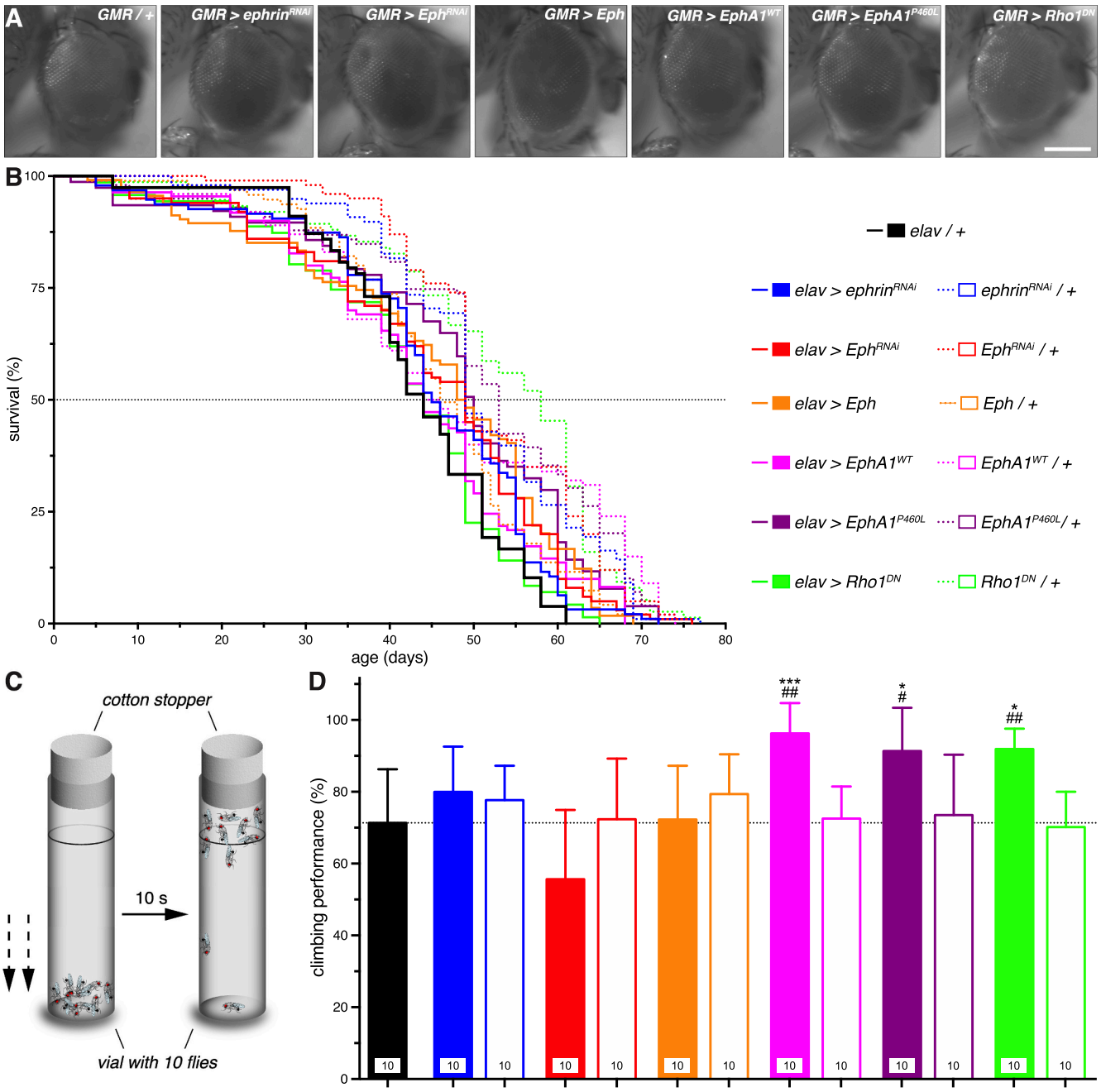

Fig. 1. Effect of Eph/ephrin manipulations on eye degeneration, lifespan and locomotor function.

(**A**) Images of compound eyes of the indicated genotypes comparing a control fly (*GMR / +*) showing the regular alignment of ommatidia to photoreceptor neurons knocking-down ephrin (*GMR > ephrin*^{RNAi}) or its receptor (*GMR > Eph*^{RNAi}), over-expressing the fiy receptor (*GMR > Eph*) or mis-expressing the human wild-type receptor (*GMR > EphA1*^{WT}), or the mutated version (*GMR > EphA1*^{P460L}) as well as a dominant negative form of Rho1 (*GMR > Rho1*^{DN}). None of the genotypes displayed a "rough eye" phenotype that would indicate neurodegeneration. Scale bar, 0.2 mm.

(**B**) Lifespan, plotted as proportion of surviving flies over time, of mated female flies kept at 25 °C, 70% humidity and 12 h:12 h light:dark (LD) cycles. Mis- and over-expression, down-regulation or dominant negative blockade of Eph/ephrin genes or Rho1 across the nervous system (using *elav-Gal4*, colour-coded as indicated) caused no significant change in lifespan compared to both *Gal4* (black solid line) and *UAS* controls (colour-coded dashed lines) using the log rank (Mantel-Cox) test ($n \geq 71$ flies per genotype).

(**C**) Cartoon depicting the negative geotaxis climbing reflex used to quantify motor deficits. Groups of 10 young male flies were gently tapped to the bottom and the number of flies reaching the line within 10 s counted.

(**D**) Flies that mis-expressed human wild-type or mutated EphA1 as well as *Rho1*^{DN} fiies showed increased performance compared to both *Gal4* (black bar) and *UAS* controls (open bars).

Bars, means; whiskers, SD; n = 10 groups of 10 flies each; $^{\#}$ $p < 0.05$, **, $^{\#\#}$ $p < 0.01$, *** $p < 0.001$; one-way ANOVA with Sidak's post hoc test compared to *Gal4* (*) and to respective *UAS* controls ($^{\#}$); detailed data in **Supplementary Table S1**, see also Fig. S2.

2.3. Eph/ephrin signalling disrupts memory formation and calcium handling

The most prominent early feature of AD dementia is memory loss (Lane et al., 2018), and we therefore tested the effect of Eph/ephrin manipulation in the *Drosophila* memory centre, the mushroom body (MB), on associative memory. Eph and ephrin are expressed in the MB (Boyle et al., 2006) and MB-wide (*OK107-Gal4*) mis-expression of human Tau and Aβ42 reduced 1 h intermediate memory (Higham et al., 2019a), assessed using the olfactory shock assay (Fig. 2A). While nave wild-type fiies consistently avoided a previously shocked odour resulting in a performance index (PI) score of 0.41, we found that MB-wide knock-down of ephrin (0.21, *UAS* 0.42) and $Rho1^{DN}$ (0.25, *UAS* 0.46) caused a reduction in memory compared to both parental controls (Fig. 2B and **Supplementary** Table S2). Neither knock-down nor over/mis-expression of either receptor caused a signiffcant reduction in memory. For fiies to successfully perform this memory task, they must be able to detect and respond normally to both the electric shock and the odours. To test the fiies' response to these sensory cues we performed control experiments that demonstrated a normal sensory response for all tested genotypes (Supplementary Fig**.** S2 and **Supplementary** Table S2). Therefore, the signiffcant reduction in memory seen for MB expression of $ephrin^{RNAi}$ and $Rho1^{DN}$ veriffes this to be a bona ffde memory defect and not attributable to a

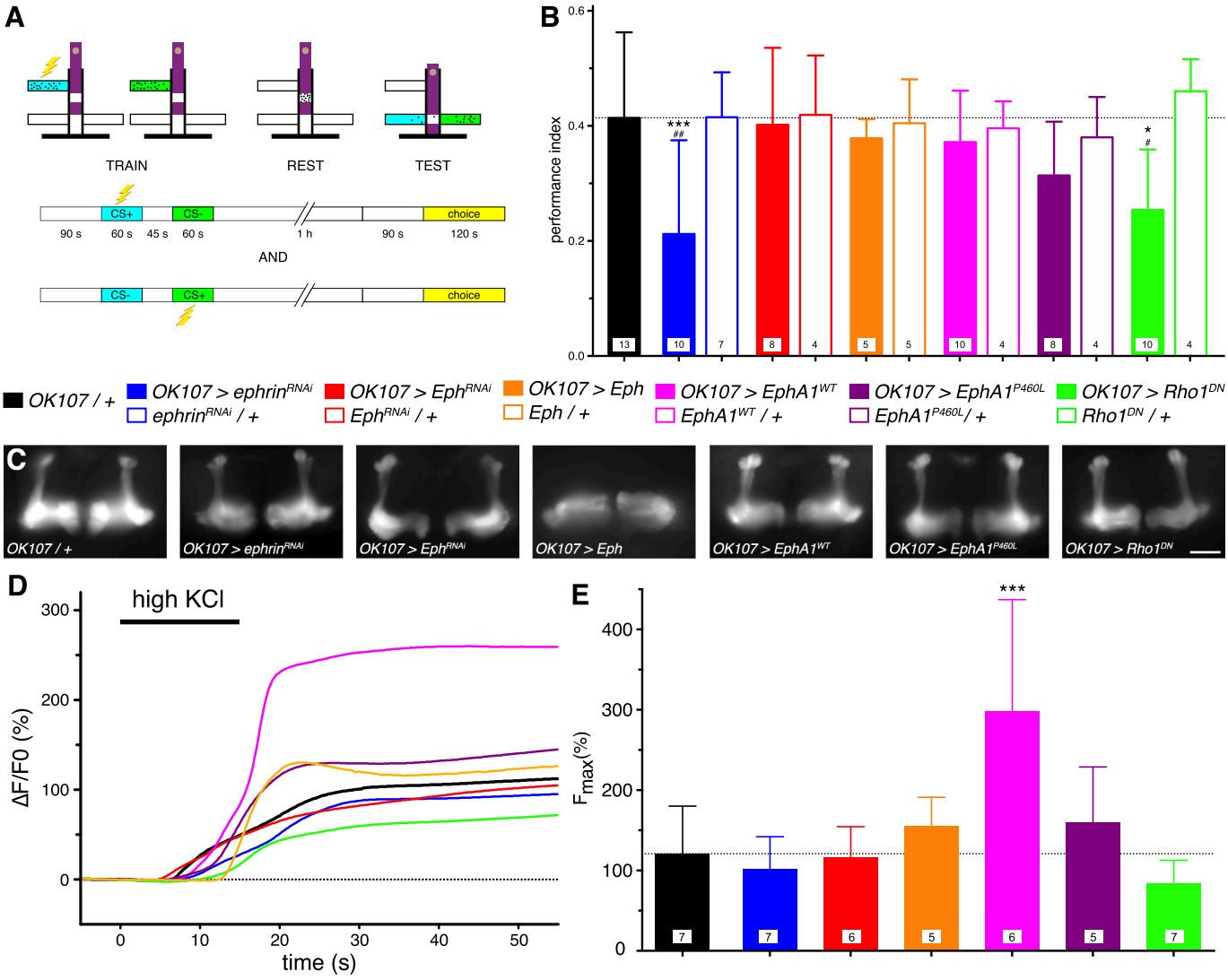

Fig. 2. Eph/ephrin signalling disrupts olfactory memory and Ca^{2+} handling.

(**A**) Schematic of the memory paradigm using the olfactory shock-conditioning one-hour memory assay. Each experiment comprised separate runs (25–50 fiies each) for both shocked odours (CS+) and the performance index calculated as the average of these.

(**B**) The aversive memory performance index scores for flies with manipulated Eph/ephrin levels in the MB (*OK107-Gal4*, colour-coded as indicated). Flies expressing $ephrin^{RNAi}$ (solid blue bar) and $Rho1^{DN}$ (solid green bar) showed reduced performance compared to both *Gal4* (black bar) and *UAS* controls (open bars). Expression of the other transgenes (Eph^{RNAi}, *Eph*, $EphA1^{WT}$, $EphA1^{P460L}$) resulted in fiies with a memory performance equivalent to that of control animals, as did the *UAS* controls. Bars, means; whiskers, SD; n, numbers in bars are number of experiments with >50 flies each; $^{\#}$ $p < 0.05$, ** $p < 0.01$; one-way ANOVA with Sidak's *post hoc* test compared to *Gal4* (*) and respective *UAS* controls ($^{\#}$).

(**C-E**) Ca^{2+} imaging of mushroom body neurons expressing the Ca^{2+} reporter GCaMP (*OK107-Gal4; UAS-GCaMP6f*).

(**C**) Images of representative mushroom bodies of young flies showed an abnormal morphology with missing α- and α'-lobes for flies over-expressing fly Eph (*OK107 > Eph*) compared to controls and no gross anatomical difference for the other genotypes (as indicated). Scale bar, 100 μm.

(**D**) Unspecific neuronal excitation by application of 100 mM KCl (black bar) led to a stronger increase in fluorescence (ΔF/F0) for $EphA1^{WT}$ fiies (magenta line). Average responses shown, for n see numbers in bars in E.

(**E**) Quantitative analysis of the maximal response (F_{max}) showed an increased responsiveness for $EphA1^{WT}$ mis-expression (magenta bar).

Bars, means; whiskers, SD; n, numbers in bars; *** $p < 0.001$; one-way ANOVA with Dunnett's *post hoc* test; detailed data in **Supplementary Table S2**, see also Fig**.** S3.

peripheral deffcit.

We have previously shown that changes in MB neuronal excitability and Ca^{2+} handling are associated with the observed memory loss (Higham et al., 2019a; Higham et al., 2019b). We thus expressed the genetically encoded Ca^{2+} sensor GCaMP6f in the mushroom body using the same promoter as for the memory experiments (*OK107-Gal4*) and measured the response of whole *ex vivo* brains to stimulation by bath-application of 100 mM KCl, that acutely depolarises and excites neurons. The axons of the so targeted MB neurons form a set of bilaterally symmetrically α, β, γ, α', and β' lobes that can be visualised by their low basal Ca^{2+} fiuorescence levels. Conffrming earlier reports (Boyle et al., 2006), we found a disturbance of the MB neuronal architecture for over-expression of fiy Eph with missing dorsal (α and α') lobes (Fig. 2C). All other genotypes appeared to have intact MB gross morphology including all lobes being present. KCl mediated neuronal depolarisation resulted in a robust and rapid increase in fiuorescence compared to baseline (ΔF/F0), this was followed by a long-lasting plateau after the maximum was reached (F_{max}, 121% for controls). This was seen in all genotypes, thereby demonstrating an excitation of this large population of neurons (Fig. 2D, E and Supplementary Table S2). However, while the manipulations resulting in memory loss, *ephrin*^{RNAi} and *Rho1*^{DN}, showed only a small reduction in the Ca^{2+} signal (F_{max} 117% and 84%), mis-expression of the human receptor *EphA1*^{WT}, on the other hand, resulted in a signiffcantly larger response with a more than doubled maximum intensity (F_{max} 299%) compared to controls. Although not signiffcant, *EphA1*^{P460L} mis-expression and fiy Eph over-expression also led to an increased Ca^{2+} signal with a F_{max} of 160% and 155% respectively. In conclusion, knock-down of ephrin and *Rho1*^{DN} lead to a memory defect, Eph over-expression to MB deformity and mis-expression of *EphA1*^{WT} resulted in an increase in neuronal excitability suggesting a role for Eph/ephrin signalling in learning and memory and the underlying MB neuronal circuits.

2.4. Eph/ephrin signalling affects activity, sleep and circadian behaviour

It is now established that circadian and sleep dysfunction is a common symptom of AD that accelerates pathology and clinical symptoms, with poor sleep being a prodromic and potential diagnostic feature for the disease with therapeutic potential (Videnovic et al., 2014; Fifel and Videnovic, 2021). We have previously shown that mis-expressing human Tau led to increased locomotor activity, reduced sleep and a weakened circadian rhythm (Buhl et al., 2019). Eph and ephrin are expressed in clock neurons (Kula-Eversole et al., 2010), therefore to determine their effects on circadian behaviour and sleep, we assessed locomotor activity utilising the *Drosophila* activity monitor (DAM) system employing the *timeless* driver (*tim-Gal4*) driving expression throughout the circadian clock (Fig. 3A). We exposed individual male fiies ffrst to a 12 h:12 h light:dark (LD) regime for 5 days before releasing them into constant dark conditions (DD) for a further 5 days. We found that flies of all genotypes showed a typical fly crepuscular behaviour in LD with activity peaks around both light transitions, a siesta at noon and prolonged sleep at night (Fig. 3C, D). The overall activity, as measured by beam breaks, was higher for fiies that mis-expressed the human *EphA1*^{WT} receptor (1391 beam breaks) compared to controls (*Gal4* 929 beam breaks, *UAS* 1029; Fig. 3B and **Supplementary** Table S3). All fiies further showed an anticipatory behaviour with ramping up of activity prior to the light transitions. In the morning, the anticipation was more pronounced for *Eph* (1.47 compared to 1.30 for *Gal4* and 1.35 for *UAS* controls) and lacking in *Rho1*^{DN} (1.16, *UAS* 1.47) flies, while in the evening anticipation was stronger for *EphA1*^{WT} (1.67 compared to 1.51 for *Gal4* and 1.53 for *UAS* controls) and *EphA1*^{P460L} (1.73, *UAS* 1.56) mis-expressor lines and again weakened for *Rho1*^{DN} (1.31, *UAS* 1.51) flies (Fig. 3E, F).

Fly sleep is characterised by a prolonged period of reduced activity along with reduced responsiveness, a sleep-speciffc posture, recovery sleep following deprivation and rapid reversibility reminiscent of what is seen in human sleep. In fiies, sleep is commonly deffned as a period of inactivity lasting 5 min or longer that can be easily measured using the DAM system (Hendricks et al., 2000; Shaw et al., 2000). The sleep proffle of male wild-type fiies showed a typical siesta around noon and sleep at night that was similar for all genotypes (Fig. 3G). However, while *Rho1*^{DN} fiies showed a less pronounced siesta, both EphA1 mis-expressing and Eph over-expressing lines produced fiies showing an earlier siesta and waking up earlier at the end of the night compared to controls. The total amount of sleep was reduced for fiies that mis-expressed both *EphA1*^{WT} (887 min compared to 1003 min for *Gal4* and 1112 min for *UAS* controls) and the *EphA1*^{P460L} (947 min, *UAS* 1201) receptors (Fig. 3H and **Supplementary** Table S3). Interestingly, fiies over-expressing Eph throughout the clock slept more in the day (531 min, *Gal4* 480 min, *UAS* 491 min) and less at night (482 min, *Gal4* 523 min, *UAS* 540 min) while *Rho1*^{DN} fiies slept less in the day (413 min, *UAS* 547 min; Supplementary Fig**.** S4B, C and **Supplementary** Table S3). The sleep composition was changed for all knock-down lines (*ephrin*^{RNAi}, *Eph*^{RNAi} and *Rho1*^{DN}) showing more sleep episodes of shorter duration (i.e. sleep fragmentation) compared to controls (e.g. *ephrin*^{RNAi} 38 bouts of average 37 min duration, compared to *Gal4* 28 bouts of 48 min and *UAS* 26 bouts of 56 min controls; Supplementary Fig**.** S4D, E). In contrast, fiy Eph over-expressor fiies demonstrated the opposite phenotype, i.e. fewer (22, *UAS* control 29) and longer (56 min, *UAS* 42 min) sleep bouts. Taken together, activity and sleep are affected by manipulation of Eph/ephrin signalling with mis-expression of human *EphA1*^{WT} leading to more activity and less sleep throughout the day, with *EphA1*^{P460L} showing a similar trend, and sleep composition was affected in all other genotypes.

We next examined whether Eph/ephrin manipulations affected the circadian clock by measuring behavioural rhythmicity during 5 days of constant darkness (DD). As expected, autocorrelation analysis revealed that 75% of wild-type flies (RS 2.4) displayed a robust circadian rhythm with a period of 24.5 h demonstrating a functioning circadian clock (Fig. 4 and **Supplementary** Table S4). Interestingly, the circadian amplitude was affected by Eph/ephrin manipulations. Mis-expressing human wild-type (88%, RS 3.2) or mutant (83%, RS 3.1) EphA1 led to a stronger rhythm and more rhythmic fiies. In contrast, knock-down of ephrin (40%, RS 1.5), Eph (43%, RS 1.5) and *Rho1*^{DN} (46%, RS 1.6) resulted in fewer rhythmic fiies displaying weaker rhythms. This could be potentially due to an unidentiffed genetic background effect since their respective UAS controls showed a similar reduction. The circadian period was not affected. The observed slightly faster clock for fiy Eph over-expressing fiies (24.1 h) can probably also be attributed to background effects because the *UAS* control flies demonstrated an even greater reduction in the circadian period (23.8 h; Fig. 4B). In summary, fiies of all genotypes have a functioning circadian clock but for human EphA1 mis-expressor fiies this clock is signiffcantly stronger compared to controls.

2.5. Eph/ephrin signalling disrupts clock neuron neurophysiology

Behaviour is controlled by deffned neuronal circuits formed by individual neurons communicating via synapses that convey their activity in the form of action potentials or spikes. In the case of circadian neurons we and others have shown that there is a day/night difference in this activity with greater activity during the day than at night, both in fiies and mammals (see (Allen et al., 2017)). The electrophysiologically best characterised and accessible fiy clock neurons are the pigment dispersing factor (PDF) releasing and wake-promoting arousal large ventro-lateral neurons (l-LNv) (Parisky et al., 2008; Shang et al., 2008; Sheeba et al., 2008; Buhl et al., 2016). As we had observed some hyperarousal, circadian and sleep phenotypes for Eph/ephrin manipulations, we next tested whether this could be due to changed neurophysiological parameters in these neurons. For this we performed whole-cell current-clamp recordings from l-LNvs in the early day (ZT1–3) and early night (ZT13–15) using the same clock-wide *tim-Gal4* driver and *UAS-GFP* to visualise the neurons (Fig. 5A).

In line with previous observations (Sheeba et al., 2008; Buhl et al., 2016; Buhl et al., 2019; Smith et al., 2019), we found that the resting membrane potential (RMP) of wild-type l-LNvs was depolarised by about 4 mV (−58.1 to −54.0 mV) and the spontaneous action potential firing rate (SFR) increased from 0.5 to 2.2 Hz in the day compared to at night, while the input resistance (R_{in}), a measure of how many ion channels are open in the membrane, was not changing with time of day (Fig. 5B-E and

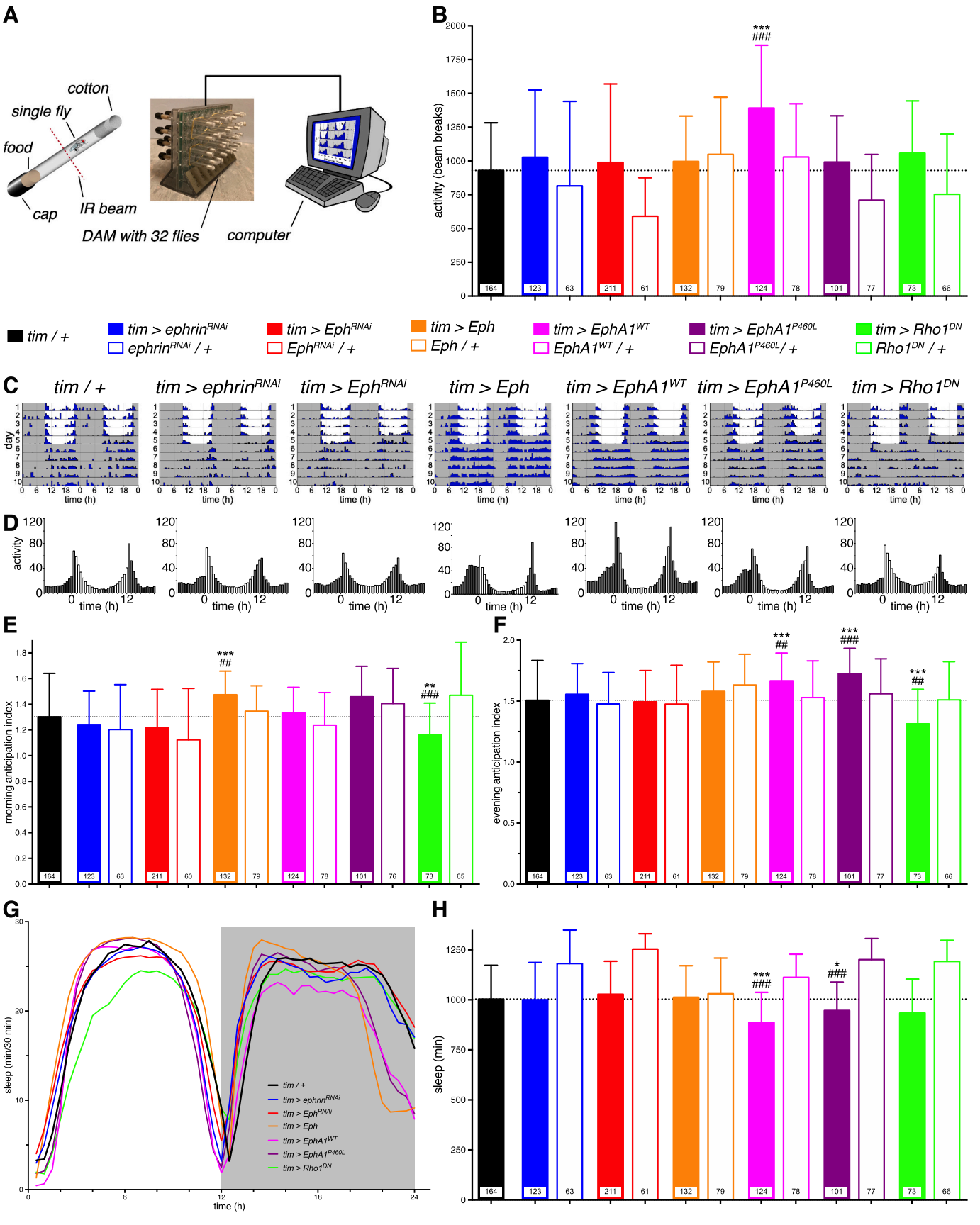

(caption on next page)

Fig. 3. Eph/ephrin signalling disrupts locomotor activity and sleep.
(**A**) Diagram of the automated fly tracking setup. Individual flies are placed in food containing tubes and loaded into a DAM monitor, where an infrared beam intersects the tube, recording when the fly travels along the tube breaking the beam. The DAM monitor is connected to a computer recording the accumulated number of beam breaks.
(**B**) Total activity levels, measured as the average daily number of beam crosses showed an increase in activity of flies mis-expressing the human wild-type receptor throughout the circadian clock (*tim* > *EphA1*^{WT}). Genotypes colour coded as indicated.
(**C**) Double-plotted actograms of exemplary flies depicting the daily activity levels of control (*tim* > +) and experimental flies (as indicated). Flies were recorded for the first 5 days in a 12 h:12 h LD cycle (grey, lights off; white, lights on) and then released in constant dark conditions for 5 days (DD).
(**D**) Histograms showing the 5-day average activity levels of all flies in LD for the same genotypes.
(**E**) Morning and (**F**) evening anticipation indices demonstrating an increased morning anticipation for fly Eph over-expressing flies and increased evening anticipation for *EphA1*^{WT} and *EphA1*^{P460L} fiies while decreased anticipation for *Rho1*^{DN} fiies.
(**G**) Sleep distribution profiles, plotted as time asleep within 30 min bins, over the day (grey, lights off; white, lights on) and (**H**) total daily sleep for the LD condition showed reduced sleep for flies mis-expressing either human EphA1 receptor. Genotypes colour coded as indicated.
Bars, means; whiskers, SD; n, numbers in bars; * $p < 0.05$, **, $^{\#\#}$ $p < 0.01$, ***, $^{\#\#\#}$ $p < 0.001$; Kruskal-Wallis with Dunn's *post hoc* test compared to *Gal4* (*) and to respective *UAS* controls ($^{\#}$); detailed data in **Supplementary Table S3**, see also Fig. S4.

Supplementary Table S5). Since neurons exchange information not just via the frequency of spike ffring but also by their ffring pattern, we calculated a ffring irregularity index (C_V) and found an increase in the night (0.53) compared to less variable ffring at day (0.28; Fig. 5F). We then assessed electrical excitability by injecting depolarising currents and measuring the resulting spiking activity to generate a frequency–current (FI) curve. We found no day/night difference for control l-LNvs at maximal injected currents ($f_{+40\ pA}$, 32.3 Hz and 30.4 Hz; Fig. 5G) but the gain of the neurons, measured as the slope of the FI curve, was stronger in the day (0.89) compared to at night (0.72; Fig. 5H).

Interestingly, most of the observed day/night differences in RMP, SFR, C_V and neuronal gain were abolished for neurons with manipulated Eph/ephrin levels or mis-expressing human EphA1, despite a seemingly functional circadian clock in these fiies (see Fig. 4). We found for all the recorded genotypes that their neurons were more depolarised at night becoming more similar to wild-type day levels. *Eph*^{RNAi} neurons were even more depolarised at day (−51.3 mV compared to −54.9 mV at night) preserving a day/night difference for this genotype (Fig. 5C and **Supplementary** Table S5). The input resistance (R_{in}) was for all genotypes measured as around 2 GΩ and did not change with time of day except for a slightly larger R_{in} of 2.25 GΩ found for *ephrin*^{RNAi} neurons at night (Fig. 5D). Nearly all neurons had an elevated SFR compared to controls both at day and at night, especially prominent for neurons over-expressing fiy Eph or mis-expressing either human EphA1 receptor (e.g. 6.24 Hz for *EphA1*^{P460L} at night; Fig. 5E). Strikingly, the day/night difference was even reversed for *Rho1*^{DN} l-LNvs with a higher ffring rate at night (3.02 Hz compared to 1.36 Hz at day). In addition to the firing frequency, the firing pattern was also affected with neurons generally firing more regularly, like wild-type neurons during the day (e.g. 0.21 for *Eph* at night; Fig. 5F). Again, the exception was *Rho1*^{DN} l-LNvs that demonstrated a more irregular ffring pattern both at day and night (0.54 and 0.46), similar to wild-type night neurons. Neuronal excitability was also affected with signiffcantly higher frequencies observed for both EphA1 mis-expressing neurons at day and night, as well as *ephrin*^{RNAi}, *Eph* and *Rho1*^{DN} neurons at night (e.g. 42 Hz for *EphA1*^{P460L} at night; Fig. 5G). Additionally, we found a day/night difference for *EphA1*^{P460L} and *Rho1*^{DN} neurons that were more excitable at night. Furthermore, the neuronal gain was higher for all recorded experimental genotypes at night and for *EphA1*^{WT} at day and, additionally, we found a reversal of the wild-type day/night difference for *EphA1*^{P460L} neurons with a higher gain at night (1.05 compared to 0.89 at day; Fig. 5H). To summarise, we found a break-down of the typical day/night differences in physiological parameters with especially *Eph*, *EphA1*^{WT} and *EphA1*^{P460L} neurons showing hyperexcitation across the day and night, and *Rho1*^{DN} neurons sometimes even reversing the wild-type day/night phenotype.

3. Discussion

We generated and characterised the ffrst animal model based on mis-expression of Alzheimer's disease (AD) associated EphA1 and non-synonymous P460L mutation (Carrasquillo et al., 2011; Hollingworth et al., 2011; Naj et al., 2011; Vardarajan et al., 2015). As there are limited treatment options for AD, there is a great need to understand the fundamental biology underlying the disease as well as to identify new targets for treatment. Harnessing the ever-increasing power of human high throughput sequencing has already identiffed 100s of potential genes involved in AD, however, confirmation of whether and how these novel genes cause pathology is lacking. Here, utilising the powerful genetic and phenotypic assays available in *Drosophila*, we successfully generated flies that allow targeted mis-expression of human wild-type *EphA1*^{WT} and mutant *EphA1*^{P460L} as well as manipulating fiy Eph/ephrin levels and showed that they changed the behaviour and physiology of the fiies. This allowed us to determine the role of Eph/ephrin signalling on neurodegeneration, lifespan, behaviour and neurophysiology.

EphA1 is the ffrst identiffed member (Hirai et al., 1987) of the large family of receptor tyrosine kinases that, when binding their endogenous ephrin ligands, allow bidirectional signalling (Lisabeth et al., 2013). While other Eph receptors and ephrins have been proposed to interact with or affect other AD risk genes like APP (Cissé and Checler, 2015) and BACE1 (Tamura et al., 2020), the role of EphA1 in AD remains unknown. So far, EphA1 has been found to affect AD and Parkinson's disease progression by regulating neuroinfiammatory processes (Villegas-Llerena et al., 2016; Ma et al., 2021) and a variant of EphA1 has been suggested to partially decrease the risk of AD in Caucasians (Wang et al., 2015). *in vitro* data suggested that the *EphA1*^{P460L} mutation might be playing a role in anchoring the EphA1 ectodomain onto the lipid bilayer leading to dimerisation and clustering, thereby promoting receptor auto-activation resulting in a constitutively active receptor (Kim et al., 2021). Therefore, we hypothesised that P460L would also have additive effects *in vivo*. However, in our fly model this is not the case as both wild-type and mutant EphA1 receptors produced very similar phenotypes.

AD is a progressive neurodegenerative disease involving multiple cellular malfunctions, synaptic and network defects eventually manifesting in a number of cognitive deffcits and ffnally contributing to early death (Lane et al., 2018). Here, we ffnd only mild behavioural and neurophysiological effects of EphA1 or disrupted Eph/ephrin signalling, thus resembling the early stages of disease progression. In *Drosophila*, it has been shown that knock-down or complete loss of Eph led to impaired olfactory learning, mushroom body (MB) defects, disrupted optic lobe development and axonal pathfinding, and enhanced Tau toxicity (Bossing and Brand, 2002; Dearborn et al., 2002; Boyle et al., 2006; Dearborn et al., 2012; Dourlen et al., 2017). While an earlier report, using a different RNAi line combined with *Dicer2*, suggested a mild rough eye phenotype for Eph (Iyer et al., 2016) and over-expression of fiy ephrin caused more severe rough eyes (Dearborn et al., 2012), we did not ffnd degeneration of the eye with neither *Eph*, *EphA1*^{WT}, *EphA1*^{P460L}, *Eph*^{RNAi}, *ephrin*^{RNAi} nor *Rho1*^{DN} (Fig. 1). However, gross MB morphology was affected in our fiy Eph over-expressor fiies that lacked both α and α' lobes (Fig. 2). Misguided or lost individual axons, particularly in the dorsal MB lobes, have been reported for Eph/ephrin signalling before (Boyle et al., 2006). The same study also found similar defects for Eph and ephrin null mutants, however, we did not observe any abnormality with our RNAi lines. This may be because our experiments were performed with targeted knock-

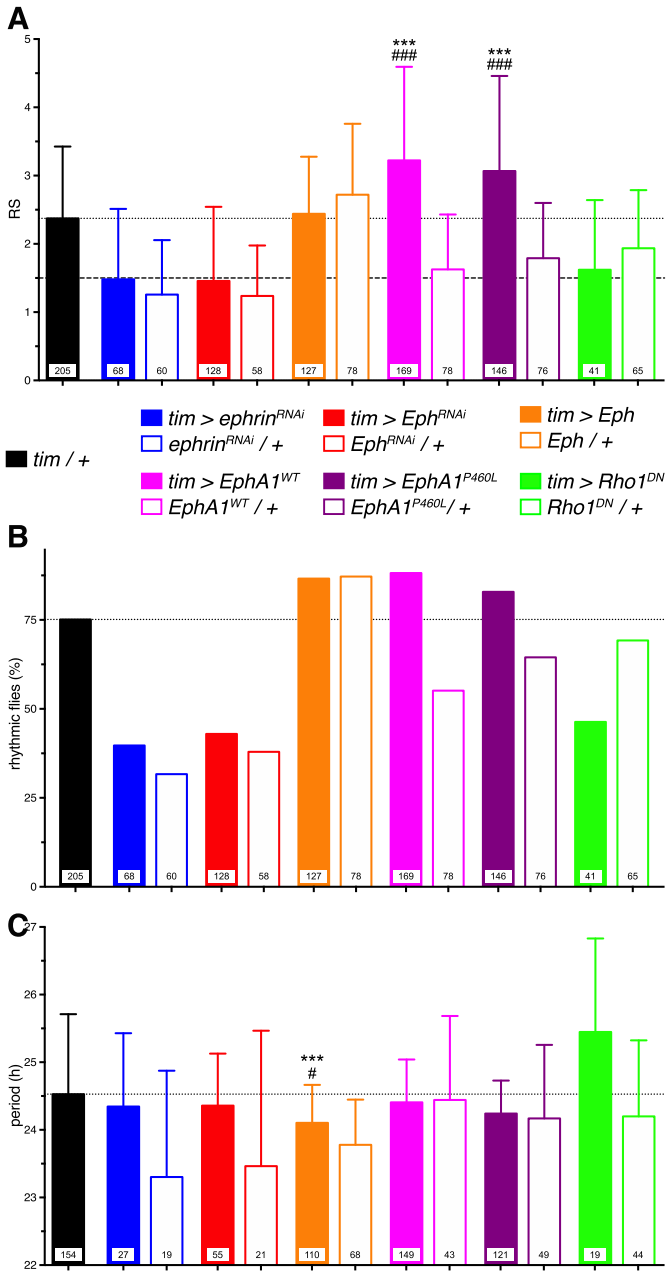

Fig. 4. Eph/ephrin effects on circadian behaviour.
(**A**) Circadian rhythm strength (RS, rhythmic for RS > 1.5 as indicated by dashed line), (**B**) percentage of rhythmic flies and (**C**) circadian period length for the same flies as in Fig. 3, recorded in constant dark conditions for 5 days (DD). *EphA1*^{WT} and *EphA1*^{P460L} flies had a stronger rhythm and more rhythmic flies compared to both *UAS* and *Gal4* control flies. *Eph*^{RNAi}, *ephrin*^{RNAi} and *Rho1*^{DN} knock-down resulted in flies with a reduction in rhythmicity albeit not signiffcantly different to their respective *UAS* controls. Over-expression of fly endogenous Eph (*tim* > *Eph*) reduced the circadian period but even more so for their *UAS* controls (*Eph* / +). Genotypes colour coded as indicated.
Bars, means; whiskers, SD; n, numbers in bars; $^{\#}$ $p < 0.05$, ***, $^{\#\#\#}$ $p < 0.001$; Kruskal-Wallis with Dunn's *post hoc* test compared to *Gal4* (*) and to respective *UAS* controls ($^{\#}$); detailed data in **Supplementary Table S4**.

down and hence partial loss of function of the genes restricted to the MB only, with the RNAi lines we used showing 54% (*Eph*^{RNAi}) and 34% (*ephrin*^{RNAi}) knock-down. This could account for the discrepancy especially since Boyle et al. reported that heterozygotes did not produce a phenotype (Boyle et al., 2006). Interestingly, we did not see a MB defect for mis-expressing human EphA1 suggesting that the human receptor might act differently in this developmental setting.

While the lack of a clear neurodegeneration phenotype could be attributed to using young animals in our assays, however, it should be noted that longevity was not affected in any of the tested genotypes (Fig. 1). This suggests that Eph/ephrin may disturb neuronal function independent of degeneration and aging. We thus tested memory, a hallmark of AD, and found that *Rho1*^{DN} and knock-down of the ligand ephrin in the MB, but not of the receptor Eph, resulted in memory impairment (Fig. 2). Likewise, over-expression of fiy or mis-expression of the human EphA1 receptors also had no effect. Nevertheless, together with the observed MB defects for Eph fiies, our results suggest a role for Eph/ephrin in associative memory, possibly more pronounced in long-term memory as shown for the alpha-lobes-absent mutants (Pascual and Préat, 2001). Similarly, blocking Eph/ephrin signalling resulted in memory deffcits in bees (Vidovic et al., 2007) suggesting a conserved mechanism across species.

A striking phenotype we observed was fiies with pan-neuronal mis-expression of EphA1 displaying hyperarousal, while clock-wide mis-expression increased locomotor activity and reduced sleep, enhanced anticipation of light transitions and strengthened behavioural rhythms (Figs. 3 and 4). This hyperarousal phenotype is shown in the better and long-lasting climbing performance seen in these fiies (Fig. 1). However, over-expression of fiy Eph did produce neither hyperarousal nor more activity, but these fiies also showed a pronounced increase in anticipatory behaviour especially in the morning. While the total amount of sleep was not affected, sleep composition was altered. *Eph* flies slept more at day and less at night with fewer but longer sleep bouts. Remarkably, *Eph*^{RNAi}, *ephrin*^{RNAi} and *Rho1*^{DN} fiies showed the opposite phenotype with more fragmented sleep. Interestingly, we have previously shown that fiies mis-expressing human Tau also exhibited greater locomotor activity and displayed a loss of sleep with altered composition (Buhl et al., 2019). Furthermore, fiies mis-expressing Aβ42 showed reduced and fragmented sleep (Tabuchi et al., 2015). As with Tau mis-expressing fiies, sleep reduction was especially pronounced at night recapitulating what is reported in AD and other neurodegenerative diseases (Fifel and Videnovic, 2021). Contrasting the Tau and Aβ42 fiies that also show a circadian dysfunction (Chen et al., 2014; Buhl et al., 2019), *EphA1*^{WT} and *EphA1*^{P460L} fiies are rhythmic in DD and show an even stronger rhythm than wild-type suggesting that their circadian clock is not affected (Fig. 4).

Corresponding to the hyperarousal phenotypes and increase in anticipatory behaviour we observed in EphA1 mis-expressing fiies, we also found neurophysiological abnormalities in these fiies which had more active and excitable clock neurons (Fig. 5). The PDF releasing LNvs are obvious candidates to underlie these phenotypes as they promote arousal (large LNv) and are required for correct morning anticipation (small LNv) (Grima et al., 2004; Stoleru et al., 2004; Parisky et al., 2008; Gmeiner et al., 2013). We found a breakdown of the typical day/night difference in physiological parameters, with higher ffring rates and a greater excitability especially for *Eph*, *EphA1*^{WT} and *EphA1*^{P460L} large LNvs both at day and particularly at night. These neurons also exhibited a higher neuronal gain, again especially at night. This changes the computational properties of the neurons leading to a, potentially inappropriately, stronger response to their synaptic inputs. This could explain the reduced sleep (particularly at night) and may result in a lower arousal threshold leading to the higher morning anticipation (MAI) and general hyperarousal observed in these animals. Supporting this neuronal over-excitation, we also found a stronger Ca^{2+} response in the MB particularly for *EphA1*^{WT} fiies (but also increased for *Eph* and *EphA1*^{P460L}), however, we did not ffnd that this affected memory retention (Fig. 2), suggesting that other circuits, beside clock neurons may also be affected. Disrupted Ca^{2+} handling in fiies has also been reported for Tau, Aβ42 and Ankyrin, however, in these cases it was accompanied by memory defects (Higham et al., 2019a; Higham et al., 2019b). Similarly, large LNvs mis-expressing human Tau were found to ffre more throughout the day and night, again likely underlying their hyperarousal phenotype (Buhl et al., 2019). Interestingly, these neurons were found to still had a day/night difference in activity and did not show an increase in neuronal excitability. Knock-down of endogenous Eph or ephrin also resulted in altered large LNv properties but to a lesser extent. We would expect those neurophysiological effects to not to be limited to the large LNvs but to affect the whole clock network. This could lead to altered overall activity or timing of

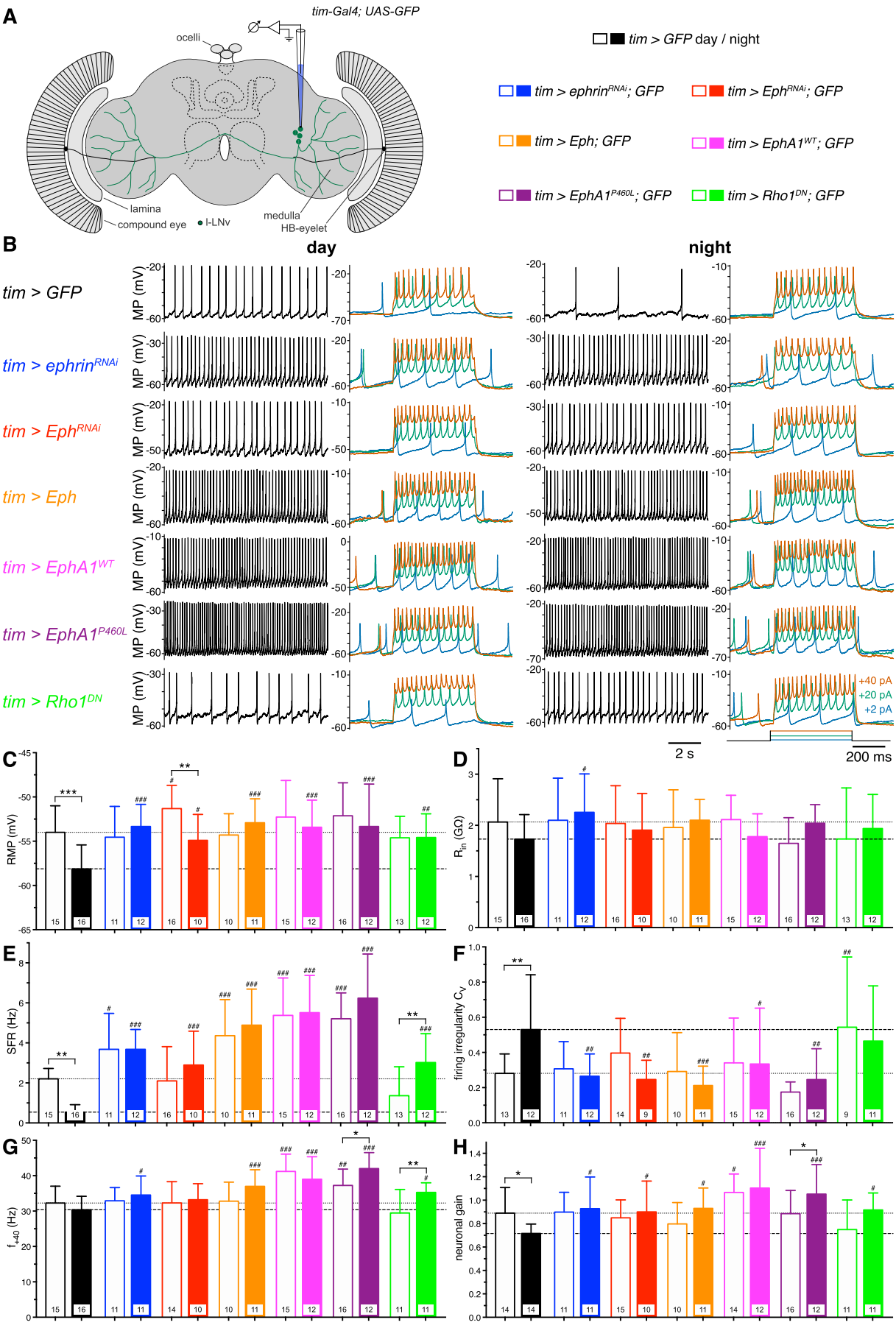

(caption on next page)

Fig. 5. Neurophysiological properties of Eph/ephrin manipulated neurons.
(**A**) Cartoon of the fly brain and recording setup indicating the morphology of the recorded large LNv on one side visualised by GFP-expression, some brain structures indicated for orientation.
(**B**) Whole-cell current clamp recordings of l-LNv spontaneous activity (left panels) and response to a current pulse (right panels, colour-coded as indicated) of control (*tim > GFP*) and manipulated l-LNvs recorded at day (ZT1–3, left side) and night (ZT13–15, right side). MP, membrane potential.
(**C**) Resting membrane potential (RMP), (**D**) input resistance (Rin), (**E**) spontaneous firing rate (SFR), (**F**) firing irregularity (C_V), (**G**) firing rate at +40 pA injected current (f_{+40}) and (**H**) neuronal gain of control (black bars) and experimental (coloured bars) l-LNv at day (open bars) and night (solid bars). Generally, experimental neurons showed less pronounced day to night differences and were more like wild-type day recordings. Especially *Eph*, *EphA1*^{WT} and *EphA1*^{P460L} neurons were ffring more and more excitable than controls.
Bars, means; whiskers, SD; n, numbers in bars; *, $^{\#}$ $p < 0.05$, **, $^{\#\#}$ $p < 0.01$, ***, $^{\#\#\#}$ $p < 0.001$; two-way ANOVA with Fisher's *post hoc* test for day/night comparison within each genotype (*) and respective comparison to corresponding day or night *tim > GFP* controls ($^{\#}$); detailed data in **Supplementary Table S5.**

activity in the clock and changes in synaptic communication between clock components. Since we also found effects on the circadian rhythm, we speculate that the small LNvs, important for DD rhythmicity and morning anticipation, are similarly affected by these manipulations. Pertinent to this, both Eph and ephrin have been shown to be important for synapse formation and activity-dependent plasticity (Lai and Ip, 2009), suggesting different underlying neurophysiological mechanisms for Eph/ephrin knock-down and EphA1 or Tau mis-expression.

In order to ffnd potential mechanisms of action of Eph/ephrin signalling, we looked at possible intracellular targets and interacting partners. The small GTPase RhoA is a major intracellular effector of EphA1, known to be activated by it (Yamazaki et al., 2009). We wanted to verify if this interaction occurred in fiies. Therefore, we anticipated to ffnd phenotypes similar to *Eph*^{RNAi} and opposite to those found for *Eph*, and possibly *EphA1*^{WT} and *EphA1*^{P460L}, when blocking the function of its fiy homologue, Rho1, by expressing the dominant negative transgene. Indeed, *Rho1*^{DN} fiies showed less anticipation, slept less at day, had fragmented sleep and a neurophysiology more like *Eph*^{RNAi} as opposed to *Eph* neurons. Reinforcing Rho1's involvement in the circadian clock, over-expression of Rho1 has been shown to lock the axonal termini of the small LNv key clock neurons in a simple/closed dusk-like state (Petsakou et al., 2015), thus limiting neuronal plasticity. Intriguingly, Eph/ephrin signalling and thus Rho activity is involved in synapse formation and activity-dependent plasticity (Lai and Ip, 2009) that could underlie the observed change in anticipatory behaviour for *Eph*, *EphA1*^{WT} and *Rho1*^{DN} fiies, suggesting a conserved mechanism. These changes in cell morphology could also infiuence the effectiveness of communication with synaptic partners, potentially leading to the observed neurophysiological effects on neuronal excitability and activity. Fascinatingly, the large LNvs of *Rho1*^{DN} even showed a reversed day/night ffring pattern. However, *Rho1*^{DN} fiies also showed increased climbing performance similar to *EphA1*^{WT} and *EphA1*^{P460L} suggesting some other mechanism at work in this case. Underlying the observed changes in neuronal excitability and synaptic plasticity might be a compromised trafffcking and clustering of ion channels and receptors, also implicated in AD. Knock-down of L-type voltage-gated Ca^{2+} channels can rescue Tau-induced memory and MB Ca^{2+} handling deffcits (Higham et al., 2019a) and Ankyrin, that links ion channels to the cytoskeleton, also affects Ca^{2+} handling and memory (Higham et al., 2019b). Interestingly, STRING-DB protein interaction network analysis (https://string-db.org) (Szklarczyk et al., 2019) shows a close connection of Ankyrin and Eph and down-regulation of Eph enhanced Tau toxicity (Dourlen et al., 2017) suggesting an interaction. More experiments are required to investigate the nature of the interaction between Eph/ephrin, Rho1, Tau and Ankyrin. Finally, in order to investigate how the Eph/ephrin complex dysregulation may contribute to AD pathology, it will be interesting to study the role of Eph/ephrin signalling in infiammation in fiies since EphA1 is implicated in regulating neuro-infiammation, a common pathological feature of AD (Ransohoff, 2016; Villegas-Llerena et al., 2016).

In conclusion, we set out to generate fiy models of AD based on targeted mis-expression of AD-associated human EphA1 wild-type and P460L transgenes. While these fiies show some AD-relevant phenotypes such as hyper-arousal, loss of sleep and disturbed neurophysiology, we found that over-expression of fiy endogenous Eph did not mimic these phenotypes in all cases. Likewise, knock-down of fiy Eph or the intracellular target Rho1 did not always produce effects opposite to EphA1. This suggests that human EphA1 might not interact with fiy ephrin or activate the intracellular signalling cascade in the same way as fiy endogenous Eph. While these factors present a limitation of our model and highlight the need to scrutinise animal models for applicability, this is generally true for all animal disease models. Regardless, we show that Eph/ephrin signalling plays a role in locomotion, memory, sleep and circadian behaviour as well as affecting neurophysiology, potentially interacting with other AD candidate genes which also produce similar phenotypes in fiies. This study, therefore, provides a starting point for further examinations into EphA1-mediated mechanisms of AD pathology.

4. Methods

4.1. Animals

Flies were raised with a 12 h:12 h light:dark (LD) cycle with lights on at ZT0 (Zeitgeber Time) on standard *Drosophila* medium (0.7% agar, 1.0% soya flour, 8.0% polenta/maize, 1.8% yeast, 8.0% malt extract, 4.0% molasses, 0.8% propionic acid, 2.3% nipagen) at 25 °C and collected between two to five days post eclosion. The following strains were used in this study and obtained from the Bloomington *Drosophila* Stock Center (Indiana University, IN, USA) or as indicated: *UAS-ephrin*^{RNAi} (BL34614), *UAS-Eph*^{RNAi} (BL35290), *UAS-Eph* (BL59844), *UAS-EphA1*^{WT} and *UAS-EphA1*^{P460L} (this study), *UAS-Rho1*^{DN} (BL7328). For the photoreceptor degeneration assay these transgenes were expressed under the control of *GMR-Gal4* (BL9146), for longevity and climbing assays under control of *elav-Gal4* (BL8765), for memory and for Ca^{2+} imaging essays under control of *OK107-Gal4* (BL854), for circadian/sleep and neurophysiology essays under control of *tim-Gal4* (gift from Dr. Ralf Stanewsky, University of Munster, Germany); for Ca^{2+} imaging *UAS-GCaMP6f* (BL52869) and for labelling neurons for electrophysiological recordings *UAS-mCD8::GFP* (BL5137) were used; controls were generated by crossing driver and responder lines to *Canton-S w-* (gift from Dr. Scott Waddell, University of Oxford, UK). All chemicals were purchased from Sigma-Aldrich (Gillingham, UK).

4.2. Generation of mis-expressor human EphA1^{WT} and EphA1^{P460L} *Drosophila lines*

Human *EphA1* cDNA was obtained from Origene (plasmid cat# RC213689) from which the *EphA1*^{P460L} variant was generated using the GeneART™ Site-Directed Mutagenesis System (ThermoFisher Scientiffc, A13282). Human wild-type *EphA1*^{WT} and *EphA1*^{P460L} transgenes were then transferred and cloned into *pENTR™/D-TOPO* vector by TOPO® cloning (ThermoFisher Scientific, K240020). To generate *EphA1*^{WT}*-D-TOPO* and *EphA1*^{P460L}*-D-TOPO* vectors the following primers were used: Fwd-*CACCATGGAGCGGCGCTGGCCCCT*, and Rev-*TTAAACCTTATCGTCGTCATCCTTG*. The resulting entry clones were sub-cloned into the destination vector *pBID-UASC-G* (Wang et al., 2012) (gift from Dr. Brian McCabe, Brain Mind Institute at EPFL, Lausanne, Switzerland) by Gateway Cloning (ThermoFisher Scientiffc). Germline transformants were generated with *PhiC31* integrase with Chromosome II *attP40* landing site by GenetiVision. Transgene expression was confirmed by PCR and Western blot.

4.3. RT-qPCR

Relative measure of *Eph* and *ephrin* expression levels were assessed by two-step qPCR. Two- to five-day old flies were anesthetized with CO_2 and decapitated, obtaining four biological replicates with ~25 heads each. Total *RNA* was extracted from head lysates by organic phenol/chloroform method using TRIzol reagent (Invitrogen). *RNA* quantification was carried out in Nanodrop spectrophotometer (Thermo Scientific) and *RNA* integrity was checked by electrophoresis in 1% agarose gel. Samples were treated with TURBO DNA-free kit (Invitrogen) to remove genomic DNA contamination. Reverse transcription was carried out using RevertAid First Strand cDNA Synthesis Kit (Thermo Scientific) following manufacturer's instructions, with 500 ng of *RNA* as template and Oligo(dT) as primer to amplify total *mRNA*. *cDNA* samples were stored at −20 °C or used immediately for qPCR reactions.

Quantitative PCR reactions were carried out in QuantStudio 3 Real-Time PCR system (Applied Biosystems) using HOT FIREPol EvaGreen qPCR Mix Plus (Solis BioDyne). The primers used to amplify *Eph mRNA* were as follows: *Eph*-Fwd 5'-*GAGATCAGGGCGCTTGTATT*-3′ and *Eph*-Rev 5'-*TTTCTCTTCCCGTAGGTGTTTC*-3′ with a PCR product expected size of 111 bp and for *ephrin mRNA*: *ephrin*-Fwd 5'-*TGGTGGAAGCAGGGATAGA*-3′ and *ephrin*-Rev 5'-*ATGGCTGAGGCGAAGATAAC*-3′ with a PCR product expected size of 96 bp. As a housekeeping gene, the following primers for *Actin mRNA* were used: *Actin*-Fwd 5'-*GTGTGCAGCGGATAACTAGAA*-3′ and *Actin*-Rev 5'-*ATCCGTTGTCGACCACTAAAG*-3′. The expected PCR product size was 112 bp. To activate DNA polymerase, a first step of 15 min at 95 °C was used, followed by 50 cycles of 30 s at 95 °C, 30 s at 60 °C, followed by a 1 min 72 °C elongation step. At the end of the experiment, a temperature ramp from 60 °C to 95 °C was used for melting curve analysis and the product fit to the predicted melting curve obtained by uMelt software (Dwight et al., 2011). Quantiffcation for each genotype and each gene was carried out using the $2^{(-\Delta\Delta Ct)}$ method and data was expressed as a percentage of change.

4.4. Eye degeneration assay

Based on a previously published protocol (Higham et al., 2019b), two- to ffve-day old fiies of either sex were anesthetised by CO_2 and images of the eyes of representative fiies were taken with a Zeiss AxioCam MRm camera attached to a stereomicroscope (Zeiss SteREO Discovery.V8, 8× magniffcation).

4.5. Longevity/survival assay

Two days after eclosion ten mated females were transferred to a vial containing standard food and maintained at 25 °C and 70% humidity throughout. Only mated females were used since the activity of the larvae prevents the food from drying out too quickly. For each genotype at least eight concurrent replicates were used. Flies were transferred to fresh food and deaths scored every two days as previously published (Higham et al., 2019b).

4.6. Negative geotaxis climbing assay

Ten two-day old male fiies were collected and acclimatised in the test vial for 30 min at 25 °C and experiments performed during the day (ZT2–3). Only male fiies were used to avoid any potential gender effect on this assay. Using the negative geotaxis refiex of *Drosophila*, flies were gently tapped to the bottom and the number of flies counted that climbed to above 7 cm within 10 s. For each genotype ten replicates were used and climbing performance was calculated as the average percentage of flies meeting these criteria. These experiments were repeated with the same flies once every week for 5 weeks, based on a previously published protocol (Lowe et al., 2019). Between experiments fiies were regularly transferred to fresh food.

4.7. Aversive olfactory conditioning assay

Olfactory memory experiments were carried out at 25 °C and 70% relative humidity under dim red light during the day (ZT2–7) in an environmentally controlled room as described previously (Higham et al., 2019a). Briefiy, groups of 25–50 two- to ffve-day old fiies of either sex were transferred into training tubes lined with an electriffable grid. After acclimatisation for 90 s, flies were exposed to either 3-octanol (OCT) or 4-methylcyclohexanol (MCH), the conditioned stimulus (CS+), paired with twelve electric shocks (70 V, duration 1.25 s, latency 3.75 s), the unconditioned stimulus (US), over a 60 s period. Following a 45 s rest, flies were exposed to the reciprocal odour (CS-) for 60 s with no electric shock. The odours were diluted in mineral oil to a concentration that the flies found equally aversive.

Memory retention was then tested one-hour post-conditioning (intermediate-term memory) in a T-maze with one arm exposed to CS+ and the other to CS-. Following acclimatisation for 90 s, the number of flies choosing each arm within 120 s was counted and memory quantified as the performance index (PI) using the formula:

$$PI = \frac{N_{CS-} - N_{CS+}}{N_{CS-} + N_{CS+}}$$

where N_{CS-} and N_{CS+} is the number of fiies choosing CS- and CS+, respectively. A PI = 1 indicates perfect memory where all flies chose CS-, and PI = 0 indicates a 50:50 split between CS- and CS+ and, therefore, no memory. To account for any innate bias the flies may have to an odour, the CS+ odour was reversed in alternate groups of flies and the performances from these two groups averaged to give n = 1. Further, the order of delivery of CS+ and CS- was alternately reversed. Control experiments were performed to show that the different genotypes of flies could respond to MCH, OCT and shock alone. For the latter, flies were introduced into the shock chamber and allowed to escape to a similar non-shocked chamber. After 2 min the percentage of flies avoiding the shock was calculated as the number of flies in the non-shocked chamber divided by the total number of flies times 100. Similarly, odour acuity was tested for OCT and MCH. Here, flies were given the choice of the tested odour versus air and the avoidance measured after 2 min as above.

4.8. Ca^{2+} imaging

Functional imaging was performed in the morning (ZT1–4) under red light illumination and using the genetically encoded Ca^{2+} sensor GCaMP6f as previously described (Higham et al., 2019b). Two- to seven-day old fiies of either sex were briefiy anesthetized on CO_2, decapitated and their brains dissected in extracellular saline containing (in mM): 101 NaCl, 1 $CaCl_2$, 4 $MgCl_2$, 3 KCl, 5 D-glucose, 1.25 NaH_2PO_4, 20.7 $NaHCO_3$ and adjusted to pH 7.2. Brains were held ventral side up in a recording chamber using a custom-made anchor and visualised with a 20× water-immersion lens on an upright microscope (Zeiss Examiner Z1). During the experiments, brains were continually perfused with extracellular saline (1 ml/min) and cells were depolarised by bath application of 100 mM KCl in extracellular solution for 15 s at 5 ml/min. The Ca^{2+} fiuorescence signal was obtained using a CCD camera (Zeiss Axiocam) and a 470 nm LED light source (3.04 mW/cm^2). Images were acquired at 4 fps with 10 ms exposure, recorded with ZEN (Zeiss) and plotted with Microsoft Excel. A region of interest was drawn around the mushroom bodies and mean pixel intensities measured for each time point. Change in fluorescence ($\Delta F/F_0$) was calculated relative to baseline with ΔF as fiuorescence at each time point minus baseline F_0 and expressed as percent change. As baseline (F_0) the mean fiuorescence of the 20 images (5 s) before KCl application was used. The peak fluorescence change in response to stimulation was used as a metric of transient Ca^{2+} increase.

4.9. Circadian and sleep assays

Analysis of circadian locomotor and sleep activity was performed using the *Drosophila* Activity Monitor system (DAM2, Trikinetics Inc., Waltham, MA, USA) as described before (Buhl et al., 2019). Individual two- to ffve-day old entrained male fiies were placed in DAM tubes with a small amount of standard food. Male fiies were used, as their behaviour is more stable in this assay while female activity varies depending on egg laying and larval activity. The DAM monitors were located inside a light- and temperature-controlled incubator (Percival Scientiffc Inc., Perry, IA, USA) where the fiy's activity was monitored for ffve days in 12 h:12 h light:dark cycles (LD) followed by five days under constant darkness (DD) at 25 °C and 70% relative humidity. Data were collected from four independent experiments for each genotype and pooled. Flies that had died before the end of the experiment were removed from the analysis.

Locomotor data was collected in 30 min bins for plotting of behavioural activity in LD and DD, the determination of rhythmic statistics (RS), a measure of the strength of the circadian behaviour, and circadian period calculations in DD that were performed using a signal-processing tool-box (Levine et al., 2002) implemented in Matlab (MathWorks, Natick, MA, USA). Autocorrelation analysis of the activity record for the ffve days in DD was performed to identify rhythmicity in the data and calculate RS, with RS $>$ 1.5 defined as rhythmic. Because RS cannot be negative, flies with a calculated RS $<$ 0 were assigned a power of 0 for subsequent analysis. Only flies with a RS $>$ 1.5 were included in determination of the circadian period.

Anticipation indices were calculated from the activity of fiies across the ffve days of LD by taking the ratio of the average activity 3 h before the light transition over the 6 h before transition. The morning anticipation index (MAI) is thus the ratio of ZT22–24 over ZT19–24 and evening anticipation (EAI) the ratio of ZT10–12 and ZT7–12.

Sleep parameters were quantiffed in MATLAB using the Sleep and Circadian Analysis MATLAB Program SCAMP (Donelson et al., 2012). Locomotor activity was collected in one-minute bins and sleep was deffned as ffve or more minutes of inactivity (Hendricks et al., 2000; Shaw et al., 2000). Activity and sleep measurements were averaged over the ffve days of LD, and further split into the day (i.e. when lights were on) and night (i.e. lights off) components. Parameters analysed were activity as number of beam crosses, time asleep, number of sleep episodes and mean sleep episode duration.

4.10. Electrophysiology

Whole-cell current clamp recordings were performed on the large ventrolateral clock neurons (l-LNv) as described previously (Buhl et al., 2016). The l-LNvs were visualised by GFP expression and brains illuminated with a 470 nm LED light source. Adult flies of either sex were collected two to six days post eclosion either at ZT1–3 (day condition) or ZT13–15 (night condition). For each genotype and time point brains from at least ffve different fiies were used.

Whole fiy brains were acutely dissected in extracellular saline and placed ventral side up in the recording chamber and neurons visualised using a 63× water-immersion lens. Recordings were performed at room temperature (20–22 °C) using glass electrodes with 8–15 MΩ resistance filled with intracellular solution (in mM: 102 K-gluconate, 17 NaCl, 0.94 EGTA, 8.5 HEPES, 0.085 $CaCl_2$, 1.7 $MgCl_2$ or 4 Mg·ATP and 0.5 Na·GTP, pH 7.2) and an Axon MultiClamp 700B amplifier, digitized with an Axon DigiData 1440A (sampling rate: 20 kHz; filter: Bessel 10 kHz) and recorded using pClamp 10 (Molecular Devices, Sunnyvale, CA, USA).

The liquid junction potential was calculated as 13 mV and subtracted from all the membrane voltages. The resting membrane potential (RMP) and the spontaneous action potential firing rate (SFR) were measured after stabilising for 1 min. Spiking regularity was tested by calculating a firing irregularity index (C_V) for spiking cells over 1 min of spontaneous activity, computed as the standard deviation of the interspike intervals (ISIs) over the mean of the ISIs. The membrane input resistance (R_{in}) was calculated by injecting hyperpolarising current steps and measuring the resulting voltage change using Ohm's law. Neuron excitability was measured by injecting a 500 ms long positive current pulse with increasing amplitude up to +40 pA and manually counting the resulting spikes. The neuronal gain was measured as the slope of the linear portion of this firing-current relationship.

4.11. Data analysis and statistics

All statistical analyses were performed using GraphPad Prism 7 (GraphPad Software Inc.) and ffgures were arranged in Adobe Illustrator (Adobe Systems Inc.). All data were scrutinised to check they met the assumptions of parametric analyses using the D'Agostino & Pearson test with alpha = 0.05, and non-parametric, rank-based alternatives were used where appropriate. Details of statistical tests used are in figure legends. Statistical levels are denoted as following *, $^{\#}$ $p < 0.05$, **, $^{\#\#}$ $p < 0.01$ and ***, $^{\#\#\#}$ $p < 0.001$. All data are presented as mean and standard deviation (SD).

CRediT authorship contribution statement

Edgar Buhl: Conceptualization, Methodology, Investigation, Writing – original draft, Writing – review & editing, Visualization, Funding acquisition. **Yoon A. Kim:** Methodology, Investigation, Writing – review & editing. **Tom Parsons:** Investigation, Writing – review & editing. **Bangfu Zhu:** Investigation, Writing – review & editing. **Ismael Santa-Maria:** Methodology, Writing – review & editing, Funding acquisition. **Roger Lefort:** Conceptualization, Methodology, Writing – review & editing, Funding acquisition. **James J.L. Hodge:** Conceptualization, Methodology, Resources, Writing – review & editing, Funding acquisition.

Declaration of Competing Interest

The authors declare no competing ffnancial interests.

Acknowledgements

We thank Drs Brian McCabe, Ralf Stanewsky and Scott Waddell for sharing fiies and reagents, and 5 anonymous reviewers for helpful comments and suggestions. This work was supported by a Leverhulme Trust grant (RPG-2016-318) and an Alzheimer's Research UK grant (ARUK-IRG2019B-003) awarded to J.J.L.H., and NIH grants (R01NS095922 and P50AG0008702) awarded to I.S-M. and NIH grant (R21AG061722) to R.L.

Appendix A. Supplementary data

Supplementary data to this article can be found online at https://doi.org/10.1016/j.nbd.2022.105752.

References

Allen, C.N., Nitabach, M.N., Colwell, C.S., 2017. Membrane currents, gene expression, and circadian clocks. Cold Spring Harbor Persp Biol 9.

Bateman, J.R., Lee, A.M., Ct, Wu, 2006. Site-speciffc transformation of *Drosophila* via ϕC31 integrase-mediated cassette exchange. Genetics 173, 769–777.

Beauchet, O., Launay, C.P., Annweiler, C., Allali, G., 2015. Hippocampal volume, early cognitive decline and gait variability: which association? Exp. Gerontol. 61, 98–104.

Bier, E., 2005. *Drosophila*, the golden bug, emerges as a tool for human genetics. Nat Rev Genet 6, 9–23.

Bossing, T., Brand, A.H., 2002. Dephrin, a transmembrane ephrin with a unique structure, prevents interneuronal axons from exiting the *Drosophila* embryonic CNS. Development 129, 4205–4218.

Boyle, M., Nighorn, A., Thomas, J.B., 2006. *Drosophila* Eph receptor guides specific axon branches of mushroom body neurons. Development 133, 1845–1854.

Brand, A.H., Perrimon, N., 1993. Targeted gene expression as a means of altering cell fates and generating dominant phenotypes. Development (Cambridge, England) 118, 401–415.

Buhl, E., Bradlaugh, A., Ogueta, M., Chen, K.-F., Stanewsky, R., Hodge, J.J.L., 2016. Quasimodo mediates daily and acute light effects on *Drosophila* clock neuron excitability. PNAS 113, 13486–13491.

Buhl, E., Higham, J.P., Hodge, J.J.L., 2019. Alzheimer's disease-associated tau alters *Drosophila* circadian activity, sleep and clock neuron electrophysiology. Neurobiol. Dis. 130, 104507.
Carrasquillo, M.M., Belbin, O., Hunter, T.A., Ma, L., Bisceglio, G.D., Zou, F., Crook, J.E., Pankratz, V.S., Sando, S.B., Aasly, J.O., Barcikowska, M., Wszolek, Z.K., Dickson, D. W., Graff-Radford, N.R., Petersen, R.C., Passmore, P., Morgan, K., Younkin, S.G., for the Alzheimer's Research UKc, 2011. Replication of EPHA1 and CD33 associations with late-onset Alzheimer's disease: a multi-Centre case-control study. Mol. Neurodegener. 6, 54.
Chen, K.-F., Possidente, B., Lomas, D.A., Crowther, D.C., 2014. The central molecular clock is robust in the face of behavioural arrhythmia in a *Drosophila* model of Alzheimer's disease. DMM 7, 445–458.
Cissé, M., Checler, F., 2015. Eph receptors: new players in Alzheimer's disease pathogenesis. Neurobiol. Dis. 73, 137–149.
Dearborn Jr., R.E., Dai, Y., Reed, B., Karian, T., Gray, J., Kunes, S., 2012. Reph, a regulator of Eph receptor expression in the *Drosophila melanogaster* optic lobe. PLoS One 7 e37303.
Dearborn Jr., R.E., He, Q., Kunes, S., Dai, Y., 2002. Eph receptor tyrosine kinase-mediated formation of a topographic map in the *Drosophila* visual system. J. Neurosci. 22, 1338–1349.
Dissel, S., Klose, M., Donlea, J., Cao, L., English, D., Winsky-Sommerer, R., van Swinderen, B., Shaw, P.J., 2017. Enhanced sleep reverses memory deffcits and underlying pathology in *Drosophila* models of Alzheimer's disease. Neurobiol Sleep Circad Rhythms 2, 15–26.
Donelson, N.C., Kim, E.Z., Slawson, J.B., Vecsey, C.G., Huber, R., Griffith, L.C., 2012. High-resolution positional tracking for long-term analysis of *Drosophila* sleep and locomotion using the "tracker" program. PLoS One 7, e37250.
Dourlen, P., et al., 2017. Functional screening of Alzheimer risk loci identiffes PTK2B as an in vivo modulator and early marker of Tau pathology. Mol. Psychiatry 22, 874–883.
Duffy, J.B., 2002. GAL4 system in *Drosophila*: a fiy geneticist's swiss army knife. Genesis 34, 1–15.
Dwight, Z., Palais, R., Wittwer, C.T., 2011. uMELT: prediction of high-resolution melting curves and dynamic melting proffles of PCR products in a rich web application. Bioinformatics 27, 1019–1020.
Fifel, K., Videnovic, A., 2021. Circadian and sleep dysfunctions in neurodegenerative disorders - an update. Front. Neurosci. 14.
Flanagan, J.G., Vanderhaeghen, P., 1998. The ephrins and Eph receptors in neural development. Annu. Rev. Neurosci. 21, 309–345.
Fritz, J.L., VanBerkum, M.F.A., 2002. Regulation of Rho family GTPases is required to prevent axons from crossing the midline. Dev. Biol. 252, 46–58.
Gmeiner, F., Kołodziejczyk, A., Yoshii, T., Rieger, D., Nässel, D.R., Helfrich-Förster, C., 2013. $GABA_B$ receptors play an essential role in maintaining sleep during the second half of the night in *Drosophila melanogaster*. J. Exp. Biol. 216, 3837–3843.
Grima, B., Chelot, E., Xia, R.H., Rouyer, F., 2004. Morning and evening peaks of activity rely on different clock neurons of the *Drosophila* brain. Nature 431, 869–873.
Hendricks, J.C., Finn, S.M., Panckeri, K.A., Chavkin, J., Williams, J.A., Sehgal, A., Pack, A.I., 2000. Rest in *Drosophila* is a sleep-like state. Neuron 25, 129–138.
Higham, J.P., Hidalgo, S., Buhl, E., Hodge, J.J.L., 2019a. Restoration of olfactory memory in *Drosophila* overexpressing human Alzheimer's disease associated tau by manipulation of L-type Ca^{2+} channels. Front. Cell. Neurosci. 13.
Higham, J.P., Malik, B.R., Buhl, E., Dawson, J.M., Ogier, A.S., Lunnon, K., Hodge, J.J.L., 2019b. Alzheimer's disease associated genes Ankyrin and Tau cause shortened lifespan and memory loss in *Drosophila*. Front. Cell. Neurosci. 13.
Hirai, H., Maru, Y., Hagiwara, K., Nishida, J., Takaku, F., 1987. A novel putative tyrosine kinase receptor encoded by the eph gene. Science 238, 1717–1720.
Hollingworth, P., et al., 2011. Common variants at ABCA7, MS4A6A/MS4A4E, EPHA1, CD33 and CD2AP are associated with Alzheimer's disease. Nat. Genet. 43, 429–435.
Ieguchi, K., 2015. Eph as a target in infiammation. Endocrine, Metabolic & Immune Disorders - Drug Targets 15, 119–128.
Iyer, J., Wang, Q., Le, T., Pizzo, L., Grönke, S., Ambegaokar, S.S., Imai, Y., Srivastava, A., Troisí, B.L., Mardon, G., Artero, R., Jackson, G.R., Isaacs, A.M., Partridge, L., Lu, B., Kumar, J.P., Girirajan, S., 2016. Quantitative assessment of eye phenotypes for functional genetic studies using *Drosophila melanogaster*. G3 6, 1427–1437.
Kim, Y., Lasso, G., Patel, H., Vardarajan, B., Santa-Maria, I., Lefort, R., 2021. Alzheimer's disease-associated P460L mutation in ephrin receptor type A1 (EphA1) leads to dysregulated Rho-GTPase signaling. bioRxiv:2021.2006.2017.448790.
Klein, R., 2012. Eph/ephrin signalling during development. Development 139, 4105–4109.
Kula-Eversole, E., Nagoshi, E., Shang, Y., Rodriguez, J., Allada, R., Rosbash, M., 2010. Surprising gene expression patterns within and between PDF-containing circadian neurons in *Drosophila*. PNAS 107, 13497–13502.
Lai, K.-O., Ip, N.Y., 2009. Synapse development and plasticity: roles of ephrin/Eph receptor signaling. Curr. Opin. Neurobiol. 19, 275–283.
Lane, C.A., Hardy, J., Schott, J.M., 2018. Alzheimer's disease. Eur. J. Neurol. 25, 59–70.
Levine, J., Funes, P., Dowse, H., Hall, J., 2002. Signal analysis of behavioral and molecular cycles. BMC Neurosci. 3, 1.
Lisabeth, E.M., Falivelli, G., Pasquale, E.B., 2013. Eph receptor signaling and ephrins. Cold Spring Harb. Perspect. Biol. 5.
Lowe, S.A., Usowicz, M.M., Hodge, J.J.L., 2019. Neuronal overexpression of Alzheimer's disease and Down's syndrome associated DYRK1A/minibrain gene alters motor decline, neurodegeneration and synaptic plasticity in *Drosophila*. Neurobiol. Dis. 125, 107–114.
Ma, J., Wang, Z., Chen, S., Sun, W., Gu, Q., Li, D., Zheng, J., Yang, H., Li, X., 2021. EphA1 activation induces neuropathological changes in a mouse model of Parkinson's disease through the CXCL12/CXCR4 signaling pathway. Mol. Neurobiol. 58, 913–925.
Naj, A.C., et al., 2011. Common variants at MS4A4/MS4A6E, CD2AP, CD33 and EPHA1 are associated with late-onset Alzheimer's disease. Nat. Genet. 43, 436–441.
Papanikolopoulou, K., Roussou, I.G., Gouzi, J.Y., Samiotaki, M., Panayotou, G., Turin, L., Skoulakis, E.M.C., 2019. *Drosophila* Tau negatively regulates translation and olfactory long-term memory, but facilitates footshock habituation and cytoskeletal homeostasis. J. Neurosci. 39, 8315–8329.
Parisky, K.M., Agosto, J., Pulver, S.R., Shang, Y.H., Kuklin, E., Hodge, J.J.L., Kang, K., Liu, X., Garrity, P.A., Rosbash, M., Griffith, L.C., 2008. PDF cells are a GABA-responsive wake-promoting component of the *Drosophila* sleep circuit. Neuron 60, 672–682.
Pascual, A., Préat, T., 2001. Localization of long-term memory within the *Drosophila* mushroom body. Science 294, 1115–1117.
Pasquale, E.B., 2008. Eph-ephrin bidirectional signaling in physiology and disease. Cell 133, 38–52.
Pasquale, E.B., 2010. Eph receptors and ephrins in cancer: bidirectional signalling and beyond. Nat. Rev. Cancer 10, 165–180.
Petsakou, A., Sapsis Themistoklis, P., Blau, J., 2015. Circadian rhythms in Rho1 activity regulate neuronal plasticity and network hierarchy. Cell 162, 823–835.
Ransohoff, R.M., 2016. How neuroinfiammation contributes to neurodegeneration. Science 353, 777–783.
Scully, A.L., McKeown, M., Thomas, J.B., 1999. Isolation and characterization of Dek, a *Drosophila* Eph receptor protein tyrosine kinase. Mol. Cell. Neurosci. 13, 337–347.
Shang, Y., Griffith, L.C., Rosbash, M., 2008. Light-arousal and circadian photoreception circuits intersect at the large PDF cells of the *Drosophila* brain. PNAS 105, 19587–19594.
Shaw, P.J., Cirelli, C., Greenspan, R.J., Tononi, G., 2000. Correlates of sleep and waking in *Drosophila melanogaster*. Science 287, 1834–1837.
Sheeba, V., Fogle, K.J., Kaneko, M., Rashid, S., Chou, Y.-T., Sharma, V.K., Holmes, T.C., 2008. Large ventral lateral neurons modulate arousal and sleep in *Drosophila*. Curr. Biol. 18, 1537–1545.
Smith, P., Buhl, E., Tsaneva-Atanasova, K., Hodge, J.J.L., 2019. Shaw and Shal voltage-gated potassium channels mediate circadian changes in *Drosophila* clock neuron excitability. J. Physiol. 597, 5707–5722.
Stoleru, D., Peng, Y., Agosto, J., Rosbash, M., 2004. Coupled oscillators control morning and evening locomotor behaviour of *Drosophila*. Nature 431, 862–868.
Szklarczyk, D., Gable, A.L., Lyon, D., Junge, A., Wyder, S., Huerta-Cepas, J., Simonovic, M., Doncheva, N.T., Morris, J.H., Bork, P., Jensen, L.J., Mering, C.V., 2019. STRING v11: protein-protein association networks with increased coverage, supporting functional discovery in genome-wide experimental datasets. Nucleic Acids Res. 47, D607–D613.
Tabuchi, M., Lone Shahnaz, R., Liu, S., Liu, Q., Zhang, J., Spira Adam, P., Wu Mark, N., 2015. Sleep interacts with Aβ to modulate intrinsic neuronal excitability. Curr. Biol. 25, 702–712.
Tamura, K., Chiu, Y.-W., Shiohara, A., Hori, Y., Tomita, T., 2020. EphA4 regulates Aβ production via BACE1 expression in neurons. FASEB J. 34, 16383–16396.
Vardarajan, B.N., Ghani, M., Kahn, A., Sheikh, S., Sato, C., Barral, S., Lee, J.H., Cheng, R., Reitz, C., Lantigua, R., Reyes-Dumeyer, D., Medrano, M., Jimenez-Velazquez, I.Z., Rogaeva, E., St George-Hyslop, P., Mayeux, R., 2015. Rare coding mutations identiffed by sequencing of Alzheimer disease genome-wide association studies loci. Ann. Neurol. 78, 487–498.
Videnovic, A., Lazar, A.S., Barker, R.A., Overeem, S., 2014. 'The clocks that time us' - circadian rhythms in neurodegenerative disorders. Nat. Rev. Neurol. 10, 683–693.
Vidovic, M., Nighorn, A., Koblar, S., Maleszka, R., 2007. Eph receptor and ephrin signaling in developing and adult brain of the honeybee (*Apis mellifera*). Devel Neurobio 67, 233–251.
Villegas-Llerena, C., Phillips, A., Garcia-Reitboeck, P., Hardy, J., Pocock, J.M., 2016. Microglial genes regulating neuroinfiammation in the progression of Alzheimer's disease. Curr. Opin. Neurobiol. 36, 74–81.
Wang, J.-W., Beck, E.S., McCabe, B.D., 2012. A modular toolset for recombination transgenesis and neurogenetic analysis of *Drosophila*. PLoS One 7 e42102.
Wang, H.-F., Tan, L., Hao, X.-K., Jiang, T., Tan, M.-S., Liu, Y., Zhang, D.-Q., Yu, J.-T., for the Alzheimer's Disease Neuroimaging Initiative, 2015. Effect of EPHA1 genetic variation on cerebrospinal fiuid and neuroimaging biomarkers in healthy, mild cognitive impairment and Alzheimer's disease cohorts. J. Alzheimers Dis. 44, 115–123.
Yamazaki, T., Masuda, J., Omori, T., Usui, R., Akiyama, H., Maru, Y., 2009. EphA1 interacts with integrin-linked kinase and regulates cell morphology and motility. J. Cell Sci. 122, 243–255.